

# The Effect of Firing Temperatures on Phase Evolution, Microstructure, and Electrical Properties of Ba(Zr<sub>0.05</sub>Ti<sub>0.95</sub>)O<sub>3</sub> Ceramics Prepared via Combustion Technique

Chittakorn KORNPOM, Theerachai BONGKARN \*

Department of Physics, Faculty of Science, Naresuan University, Phitsanulok, 65000, Thailand  
 Research Center for Academic Excellence in Applied Physics, Faculty of Science, Naresuan University, Phitsanulok, 65000, Thailand

**crossref** <http://dx.doi.org/10.5755/j01.ms.20.4.6436>

Received 13 February 2014; accepted 22 June 2014

In this work, the effects of calcination temperature (900 °C–1200 °C for 2 h–6 h) and sintering temperature (1350 °C–1550 °C for 2 h) on phase evolution, microstructure and electrical properties of barium zirconate titanate Ba(Zr<sub>0.05</sub>Ti<sub>0.95</sub>)O<sub>3</sub> (BZT) ceramics fabricated through the combustion technique were investigated. Glycine was used as fuel to reduce the reaction temperature. It was found that a single perovskite phase of BZT powders was observed from the sample calcined at 925 °C for 6 h, which was lower than the solid state reaction technique ~275 °C. The purity phase of an orthorhombic structure was observed in all ceramic samples. The average particle size (190 nm–420 nm) and the average grain size (2.9 μm–41.4 μm) increased with increased firing temperatures. The maximum theoretical density of ~96.8 % was obtained from the sample sintered at 1450 °C for 2 h. The dielectric constant at room temperature ( $T_r$ ) and the dielectric constant at Curie temperature ( $T_c$ ) increased with increased sintering temperatures up to 1450 °C and decreased thereafter. The dielectric properties corresponded to the obtained densities. The remnant polarization ( $P_r$ ) of the BZT ceramic (using the coercive electric field of 20 kV/cm) increased with increasing sintering temperature.

**Keywords:** barium zirconate titanate; combustion technique; phase evolution; perovskite structure.

## 1. INTRODUCTION

Pb(Zr,Ti)O<sub>3</sub> (PZT) materials have superior piezoelectric properties and are, therefore, widely used. Unfortunately, they are not environmentally friendly because lead oxide is toxic [1, 2]. Consequently, there are good environmental reasons to find lead-free piezoelectric ceramics with equivalent properties. Barium zirconium titanate is a lead-free ceramic which has received much attention [3]. Perhaps this material could replace lead-based materials because of its high dielectric, ferroelectric and piezoelectric properties [4]. Zr<sup>2+</sup> ions substituted at the B site in BaTiO<sub>3</sub> lattices will form a barium zirconium titanate ceramic. The electrical and structural properties of BaTiO<sub>3</sub> are altered [4]. These changes include a diffuse phase transition and relaxor ferroelectric behavior [4, 5]. Ba(Zr<sub>0.05</sub>Ti<sub>0.95</sub>)O<sub>3</sub> ceramic (abbreviated as BZT) is very interesting and has been studied due to its strong ferroelectric which exhibits large remnant polarization ( $P_r = 13 \mu\text{C}/\text{cm}^2 - 18 \mu\text{C}/\text{cm}^2$ ), small coercive field ( $E_c = 0.8 \text{ kV}/\text{cm} - 3.5 \text{ kV}/\text{cm}$ ), high dielectric constant and low dielectric loss [5, 6]. This makes it attractive for applications in multilayer ceramics capacitors and piezoelectric sensors/actuators [7].

There are several methods to fabricate BZT ceramics, such as the solid-state reaction method [5, 6], the ultrasonic ball milling technique [8] and the sol gel method [9]. When BZT ceramics are prepared by solid-state reaction, a large

particle size of around 1 μm–2 μm was obtained. The highest dielectric constant value of 14000 at Curie temperature and the remnant polarization ( $P_r$ ) of about 5.4 μC/cm<sup>2</sup> were observed [5, 6]. The calcination temperature of the solid state reaction method was reduced to 1000 °C by ultrasonic ball milling [8]. The resulting BZT powders had an average particle size of around 0.72 μm. The density and dielectric constant at room temperature (at 1 kHz) of the BZT ceramic were at the range of 75 %–78 % and 1128–1555 when sintered at 1350 °C [8]. N. Binhayeeniyi *et al.* [9] synthesized BZT ceramic using the sol gel method. The single perovskite phase of BZT powder with a particle dimension of around 0.28 μm was obtained when calcined at 1100 °C. The maximum density and dielectric constant at room temperature (at 1 kHz) of the ceramics were 5.06 g/cm<sup>3</sup> and 1361 when sintered at 1250 °C. Ceramics synthesized by the solid state reaction method uses high temperatures that result in powders that exhibit large particle size and wide particle size distribution [5, 6]. These characteristics are not desirable. The wet chemical synthesis methods produce homogenous nanosized oxides of high purity at lower reaction temperatures. Unfortunately, these methods are complicated and expensive. This makes them unsuitable for mass production [9].

In our previous work, we have been able to prepare ferroelectric ceramics using the combustion technique [10–15]. This is a simple technique and produces high quality ceramics. The combustion reaction itself produces heat that energizes the raw materials and speeds up the chemical reaction of the materials [11]. It was found that

\*Corresponding author. Tel.: +66-5596-3528, fax: +66-5596-3501.  
 E-mail address: [researchcmu@yahoo.com](mailto:researchcmu@yahoo.com) (T. Bongkarn)

the combustion technique can provide pure nanocrystalline powders [12], with a high density [13] and good electrical properties [14] using lower firing temperatures and requiring a shorter dwell time [14, 15]. However, from the a survey of the literature, the fabrication of Ba(Zr<sub>0.05</sub>TiO<sub>0.95</sub>)O<sub>3</sub> (BZT) ceramics using the combustion technique and the optimum firing conditions of this ceramic have not been previously studied. So, our aims were to prepare high density BZT ceramics employing the combustion technique and to observe effect of firing temperatures on phase evolution, microstructure, dielectric and ferroelectric properties.

## 2. EXPERIMENTAL

BZT powder was prepared by the combustion method using glycine as fuel. The raw material of BaCO<sub>3</sub> (99%), ZrO<sub>2</sub> (99%), and TiO<sub>2</sub> (99%) was weighed, and ethanol was added. The mixture was then ground by ball milling for 24 h using zirconia balls. The suspensions were dried, ground and then sieved into a fine powder. The raw powders were mixed with glycine in 1:2 ratio. Thermogravimetric analysis (differential thermogravimetry; DTG and thermogravimetry; TG) was used to determine the reactions between the uncalcined powders and the glycine. The next step was to heat the powders at various calcining temperatures (900 °C–1200 °C), using dwell time of 2 h–6 h and a heating/cooling rate of 5 °C/min. After being reground by ball milling with a 2 wt% binder solution, the calcined powders were dried, crushed and sieved again. Using 80 MPa, the material was pressed into 15 mm disks and then baked at temperatures ranging from 1350 °C–1550 °C for 2 h. The pellets were allowed to cool in a furnace. The various phases that formed and at what temperature was determined by X-ray diffraction (XRD). Scanning electron microscopy (SEM) and a transmission electron microscope (TEM) were used to image the morphologies of the calcined powders and sintered ceramics. A mean linear intercept method was used to determine average particle and grain size. Density was measured using the Archimedes method. A LCR meter was used to discover the dielectric constant and a computer controlled Sawyer-Tower circuit characterized the ferroelectric hysteresis (*P-E*) loop. Three BZT samples were used for characterizations which were repeated twice.

## 3. RESULTS AND DISCUSSION

Fig. 1 shows the DTG-TG curves used to investigate the calcination temperatures of the variously mixed powders BaCO<sub>3</sub>, ZrO<sub>2</sub>, TiO<sub>2</sub> and glycine. From the curve of the thermogravimetric analysis, it can be seen that there is a three-stage-weight loss. The first occurred between 180 °C and 280 °C and corresponds to the endothermic peak at 216 °C in the DTG curve. This phenomenon related to the decomposition reaction of glycine to ammonia, vapor and gasses as shown in Formula (1) (decomposition temperature of glycine is 262 °C [16, 17]). At temperature between 300 °C and 500 °C, there was a second weight loss which caused an endothermic peak in the DTG curve at temperature of 386 °C. Formula (2) [17] illustrates how the oxidation-reduction reaction between ammonia and NO caused water and gasses to vaporize which performed in

this stage. The energy, which was released in two stages, fueled and accelerated the chemical reaction taking place. The third weight loss (above 600 °C) which caused an endothermic peak at 813 °C was the result of the chemical reaction between BaCO<sub>3</sub>, ZrO<sub>2</sub> and TiO<sub>2</sub>. As the temperature reached 910 °C, its weight loss was reduced to 28.13 % of its original weight. It can be inferred that the decomposition processes of glycine and the chemical reaction of raw materials were successful because their weight loss is close to the total of the weight of glycine (66.66 %) and the weight of CO<sub>2</sub> (5.21 %) produced from the chemical reaction. Based on these results, it was estimated that the calcination temperature started at 900 °C.

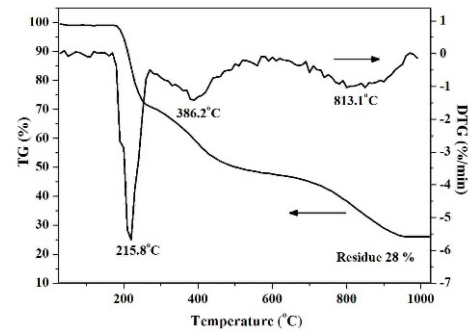


Fig. 1. DTG-TG curves for the mixture of BZT powders and glycine

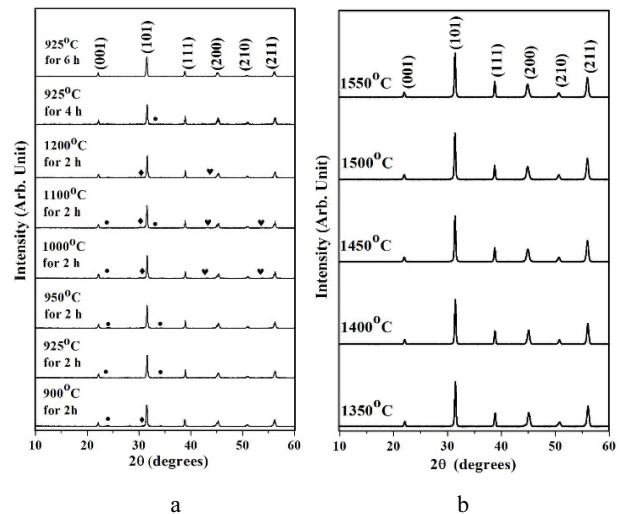


Fig. 2. The XRD patterns of BZT powders calcined at 900 °C–1200 °C for 2 h–6 h (a) and the XRD patterns of BZT ceramics sintered at various temperatures for 2 h (b): (●) BaCO<sub>3</sub>, (◆) BaZrO<sub>2</sub> and (♥) TiO<sub>2</sub>

Fig. 2, a, shows the X-ray diffraction results of BZT powders calcined between 900 °C and 1200 °C for 2 h. All peaks had an orthorhombic perovskite structure identical to JCPDS file no.81-2200 [18]. BaCO<sub>3</sub>, BaZrO<sub>2</sub> and TiO<sub>2</sub> were discovered in all the calcined powders. By measuring the intensity of the major XRD peaks, it was possible to determine the degrees of the perovskite phase. The percentage of the perovskite phase was determined using:

$$\% \text{ perovskite phase} = \left( \frac{I_{\text{perov}}}{I_{\text{perov}} + I_{\text{BaCO}_3} + I_{\text{BaZrO}_2} + I_{\text{TiO}_2}} \right) \times 100 . \quad (3)$$

This well-known equation is often used when preparing complex perovskites, [15].  $I_{\text{perov}}$ ,  $I_{\text{BaCO}_3}$ ,  $I_{\text{BaZrO}_2}$  and  $I_{\text{TiO}_2}$  refer to the highest intensity of the various peaks. The percentage of the perovskite phase increased from 93 % to 97 % when the calcination temperature increased to 925 °C. At higher temperatures the percentage of perovskite decreased. The BZT powders achieved 97 % of the perovskite phase when they were calcined at 925 °C for 2 h. The XRD patterns of the BZT powder calcined at 925 °C for 2 h–6 h are shown in Fig. 2, a. Increased dwell time reduces the impurity phase and when the powders were calcined at 925 °C for 6 h, the pure orthorhombic phase appeared. This temperature is ~275 °C less than that the solid state reaction method [5, 6]. The reduced calcination temperature technique was the result of the energy released by the fuel during the combustion process [15]. The XRD result corresponded with DTG-TG investigations.

The BZT powders obtained by calcination at 925 °C for 6 h were pressed into pellets and sintered from 1350 °C–1550 °C for 2 h. XRD analysis was used to examine how the phase structure of the ceramics was altered by the differing temperatures (Fig. 2, b). A single phase of an orthorhombic perovskite structure was found in all the samples. The diffraction peaks shift slightly toward high angles when the sintering temperature increased to 1400 °C. At higher temperatures, the diffraction peak shifted slightly to lower angles. The lattice parameters of the BZT orthorhombic structure were calculated by the following equation [15]:

$$\frac{1}{d^2} = \frac{h^2}{a^2} + \frac{k^2}{b^2} + \frac{l^2}{c^2} \quad (4)$$

The lattice parameters  $a$ ,  $c$  and the unit cell volume of the ceramics increased while, the lattice parameter  $b$  tended to decrease when sintering temperatures increased (Table 1). Different temperatures caused changes in the phase formation and the lattice parameters of the BZT. This is because the  $d$  spacing changes and results in variations in the lattice strain [19].

The SEM photographs are shown in Figs. 3, a–d. The BZT powders calcined at 900 °C–1200 °C for 2 h–6 h were spherical in shape with a porous surface. The narrow particle size distribution was observed at a high calcination temperature and with long dwell time. BZT particles increased in size – 190 nm–420 nm – with higher temperatures or dwell time. Fig. 4 shows typical TEM micrographs of BZT powder calcined at 925 °C for 6 h. The powder observed by TEM in a low magnification consisted of irregular shaped, agglomerated particles approximately 300 nm in diameter as seen in Fig. 4, a. Examination by both TEM and SEM showed a similar agglomerate size. When observed at a greater magnification (Fig. 4, b), the particles were shown to be spherical and less than 120 nm in size. These findings show that the combustion method is an excellent way to prepare BZT nanopowders.

The SEM micrographs of the surface of the BZT ceramics with different sintering temperatures are shown in Figs. 3, e–h. The grains are spherical and at low sintering temperature, have small and loosely bonded grains

(Fig. 3, e). The porosity decreased obviously while the grain size increased rapidly when sintering temperatures increased (Fig. 3, f). At a higher sintering temperature, the grain size expanded continuously while the pore structure collapsed, and the packing of grains was dramatically improved (Fig. 3, g). When the sintering temperature increased again, the grain boundary starts to melt and nearly was disappeared as seen in Fig. 3, h. This was caused by the evaporation of chemical compounds at these new high sintering temperatures [15]. The grain size increased from  $2.9 \mu\text{m} \pm 0.13 \mu\text{m}$  to  $41.4 \mu\text{m} \pm 1.1 \mu\text{m}$  with increasing sintering temperatures from 1350 °C to 1550 °C, whereas the porosity decreased with increasing sintering temperature.

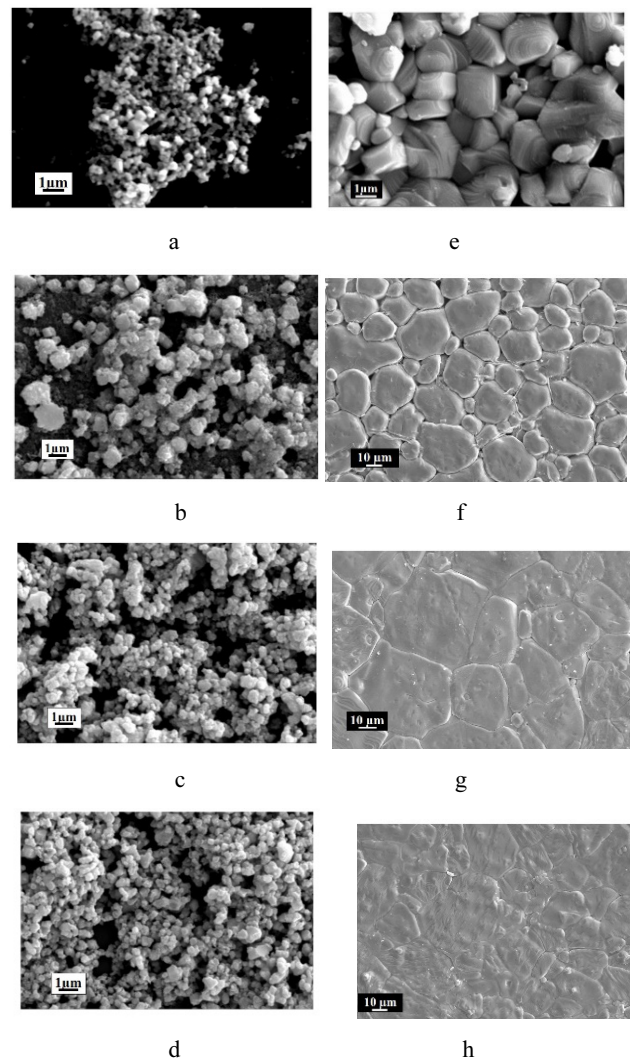


**Fig. 3.** The SEM micrographs of BZT powders calcined at 900 °C (a) and 1200 °C (b) for 2 h and calcined at 925 °C for 2 h (c) and 6 h (d) and the SEM photographs of BZT ceramics sintered at 1350 °C (e), 1400 °C (f), 1450 °C (g) and 1550 °C (h) for 2 h

The measured density and linear shrinkage are shown in Fig. 5. Density and linear shrinkage increased from  $(5.70 \pm 0.011) \text{ g/cm}^3$  to  $(5.82 \pm 0.015) \text{ g/cm}^3$  and from  $(12.32 \pm 0.03) \%$  to  $(13.48 \pm 0.025) \%$ , respectively, when sintering temperatures increased, to the maximum of 1450 °C. These densities decreased when the temperature increased above 1450 °C.

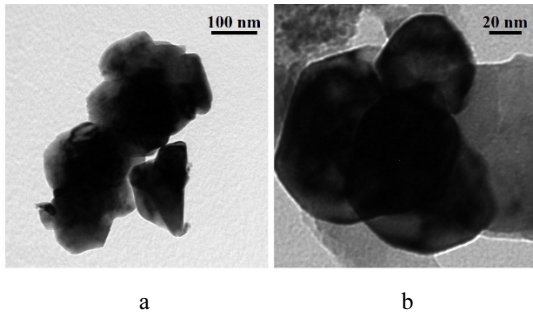


**Fig. 4.** TEM micrographs of BZT powders calcined at 925 °C for 6 h; (a) low magnification image and (b) high magnification image

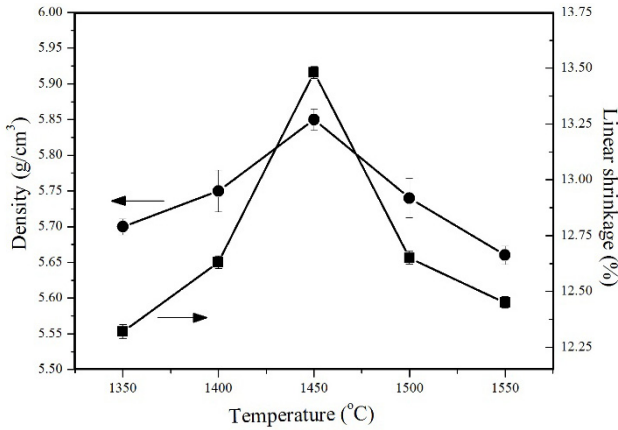


**Fig. 5.** The density and shrinkage of BZT ceramics sintered at various temperatures

The microstructure investigation showed that the density depended on the porosity and the state of the liquid phase. The liquid phase happens at higher temperatures and causes a rapid rearrangement of the particles. The grains rearrange easily when the liquid phase is at the right level, see Fig. 3, g. Because of the evaporation of the material and then inner voids form, consequently, the original high density is reduced to a lower density. It should be noted that the highest theoretical density of this work was 96.8 % (Table 1), which is higher than the samples prepared via the ultrasonic ball milling technique (~77.7 %) [8] or the sol-gel process (~90 %) [9].

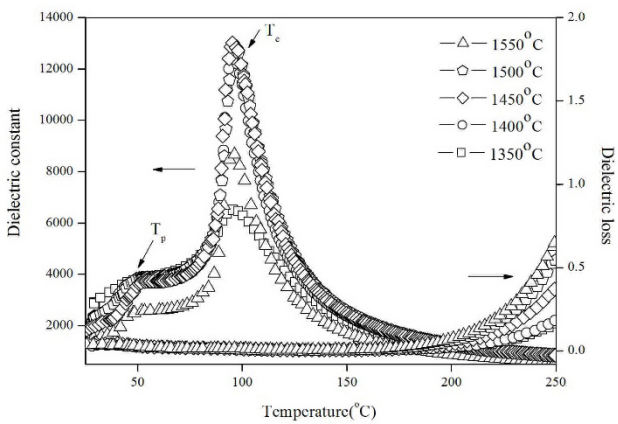


**Fig. 6.** Temperature dependence of dielectric constant and dielectric loss of BZT ceramics sintered at various temperatures

Fig. 6 shows the dielectric properties of the BZT samples measured at 1 kHz and temperatures between

25 °C and 250 °C. There were two dielectric anomalies ( $T_p$  and  $T_c$ ).  $T_p$  is the transition temperature from orthorhombic ferroelectric to tetragonal ferroelectric [19].  $T_c$  is Curie temperature and relates to the transition from tetragonal ferroelectric to cubic paraelectric [19]. The exact transition temperatures were derived from dielectric loss. The  $T_p$  and  $T_c$  were between 47.4 °C and 47.8 °C and 99.4 °C and 99.5 °C, respectively. At room temperature ( $T_r$ ), the value of dielectric constants ( $\epsilon_r$ ) tended to decrease with increasing sintering temperature (Table 1). The dielectric loss ( $\tan\delta$ ) decreased when the sintered temperature was increased to 1450 °C. Upon further increasing the temperature from 1450 °C to 1550 °C;  $\tan\delta$  increased as shown in Table 1. At the sintering temperature of 1450 °C, the sample exhibited the lowest dielectric loss of 0.031 and a dielectric constant of 2380. This was higher than the dielectric constant (~1800) at room temperature fabricated by the solid-state method [5, 6]. The dielectric constant and dielectric loss at  $T_c$  are listed in Table 1. The dielectric constant at  $T_c$  increased with increase sintering temperatures up to 1450 °C and thereafter it decreased. The dielectric properties correspond with the density result. At  $T_c$ , the highest dielectric constant of 13030 accompanied with a dielectric loss of 0.0126 was obtained in the sample sintered at 1450 °C for 2 h. The maximum dielectric constant prepared via the combustion method was higher than the samples prepared by ultrasonic ball milling technique [8] (~3000) and the sol-gel process [9] (~9000).

Fig. 7 illustrates the polarization hysteresis ( $P$ - $E$ ) loops of the BZT ceramics (using the coercive electric field of 20 kV/cm).

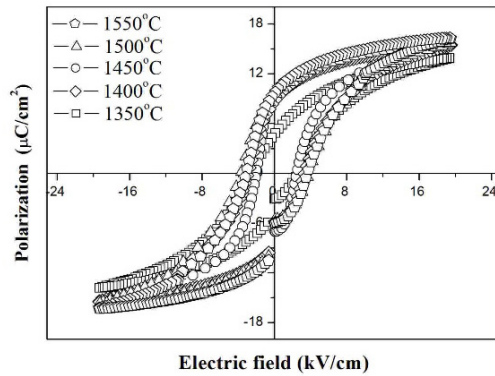


**Fig. 7.** Polarization vs. electric field of BZT ceramics sintered at various temperatures for 2 h

The result indicated that the remnant polarization  $P_r$  (the remaining polarization when an electric field decreases to zero) of the BZT ceramics increased from 4.66  $\mu\text{C}/\text{cm}^2$  to 9.64  $\mu\text{C}/\text{cm}^2$  when the sintering temperature increased from 1350 °C to 1550 °C (Table 1). The coercive field  $E_c$  (indicating an electric field required to achieve zero polarization) of the samples was between 2.54 kV/cm and 3.80 kV/cm. The lowest  $E_c$  was obtained in the ceramics sintered at 1450 °C (Table 1). Increment of  $P_r$  when sintering temperature increased may cause from the grain size effect dominate in variation of polarization [20]. W. Cao et.al. [21] established on the fact that domain size  $\alpha$  (grain size)<sup>m</sup>, where m is positive. Therefore, with the increase of grain size (with increase of sintering temperature) domain size increases, which further leads to increase in polarization.

**Table 1.** Lattice parameters, unit cell volume, average grain size, relative density, dielectric properties and ferroelectric properties of BZT ceramics

Sintered temperature (°C)	Lattice parameters (Å)			Unit cell volume (Å <sup>3</sup> )	Relative density (%)	$\epsilon_r$ at $T_r$	$\tan\delta$ at $T_r$	$\epsilon_r$ at $T_c$	$\tan\delta$ at $T_c$	$P_r$ ( $\mu\text{C}/\text{cm}^2$ )	$E_c$ (kV/cm)	$R_{sq}$
	$a$	$b$	$c$									
1350	2.1754	2.2233	2.0055	9.6973	94.0	2900	0.049	6500	0.0092	4.66	2.75	0.57
1400	2.1763	2.2236	2.0068	9.7113	94.7	2180	0.035	12600	0.0085	8.78	3.53	0.74
1450	2.1822	2.2188	2.0075	9.7200	96.8	2380	0.031	13030	0.0126	9.27	2.54	0.76
1500	2.1824	2.2160	2.0100	9.7207	95.1	1830	0.040	12700	0.0149	9.41	3.80	0.82
1550	2.1830	2.2158	2.0107	9.7259	94.2	1490	0.046	8730	0.0123	9.64	3.76	0.83

Ferroelectric characteristics can be determined by calculating the degree of squareness ( $R_{sq}$ ) of the hysteresis loop. This can be done using  $R_{sq} = (P_r/P_s) + (P_{1.1E_c}/P_s)$ , where  $P_s$  is the saturated polarization obtained at some finite field strength below the dielectric breakdown and  $P_{1.1E_c}$  is the polarization at the field equal to  $1.1E_c$ ,  $R_{sq} = 2.00$  is a perfect square loop [22]. According to this formula, the squareness of BZT samples sintered at various temperature can be calculated. The value of squareness increased from 0.57 to 0.83 when the sintering temperatures was increased from 1350°C to 1550°C. These values are listed in Table 1. This indicated that ferroelectric behavior increased with increasing sintering temperatures.

#### 4. CONCLUSIONS

Pure BZT nanopowder is successfully obtained at low calcination temperature (925°C for 6 h) using the combustion technique. The firing conditions strongly effect on phase evolution, microstructure, lattice parameters, density and the electrical properties of BZT ceramics. The BZT ceramic exhibited the pure orthorhombic phase in all samples and the lattice parameters  $a$ , and  $c$  of the ceramics increased while, lattice parameter  $b$  tended to decrease when sintering temperatures increased. At high sintering temperatures, the evaporation of chemical compounds makes the grain boundary to melt, which created low densities and poor electrical properties in the BZT ceramics. The highest relative density (96.8 %) and highest dielectric properties ( $\epsilon_r \cong 13030$  and  $\tan\delta \cong 0.0126$  at  $T_c$ ) are obtained in the sample sintered at 1450°C for 2 h. The  $P_r$  and  $R_{sq}$  increased when sintered temperature increased. The results of the microstructure, densification, and dielectric investigation complemented each other.

#### Acknowledgments

This work was financially supported by the Thailand Research Fund (TRF). Thanks also to Department of Physics, Faculty of Science, Naresuan University for supporting facilities. Acknowledgements to Mr. Don Hindle, for helpful comments and corrections of the manuscript.

#### REFERENCES

1. **Xia, Z., Li, Q.** Structural and Electrical Properties Investigations of  $\text{Pb}(\text{Mg}_{1/3}\text{Nb}_{2/3})\text{O}_3\text{-PbTiO}_3\text{-Pb}(\text{Fe}_{1/2}\text{Nb}_{1/2})\text{O}_3$  Ceramics *Scripta Materialia* 57 2007: pp. 981–984. <http://dx.doi.org/10.1016/j.scriptamat.2007.08.010>
2. **Bauger, A., Moutin, J. C., Niepce, J. C.** Synthesis Reaction of Metatitanate  $\text{BaTiO}_3$  *Journal of Materials Science* 18 1983: pp. 3041–3046. <http://dx.doi.org/10.1007/BF00700786>
3. **Wang, Y. L., Li, L. T., Qi, J. Q., Gui, Z. L.** Ferroelectric Characteristics of Ytterbium-doped Barium Zirconium Titanate Ceramics *Ceramics International* 28 2002: pp. 657–661.
4. **Yu, Z., Guo, R., Bhalla, A. S.** Dielectric Behavior of  $\text{Ba}(\text{Ti}_{1-x}\text{Zr}_x)\text{O}_3$  Single Crystals *Journal of Applied Physics* 88 2000: pp. 410–416. <http://dx.doi.org/10.1063/1.373674>
5. **Yu, Z., Ang, C., Guo, R., Bhalla, A. S.** Piezoelectric and Strain Properties of  $\text{Ba}(\text{Ti}_{1-x}\text{Zr}_x)\text{O}_3$  Ceramics *Journal of Applied Physics* 92 2002: pp. 1489–1493. <http://dx.doi.org/10.1063/1.1487435>
6. **Moura, F., Simoes, A. Z., Stojanovic, B. D., Zaghete, M. A., Longo, E., Varela, J. A.** Dielectric and Ferroelectric Characteristics of Barium Zirconate Titanate Ceramics Prepared from Mixed Oxide Method *Journal of Alloys and Compounds* 462 2008: pp. 129–134.
7. **Swartz, S. L.** Topics in Electronic Ceramics *IEEE Transactions Dielectrics Electrical Insulation* 25 1990: pp. 935–987. <http://dx.doi.org/10.1109/14.59868>
8. **Thamjaree, W., Nhuapeng, W., Tunkasiri, T.** Fabrication of Barium Zirconium Titanate Ceramics Using Ultrasonic Ball Milling Technique *Advanced Materials Research* 55–57 2008: pp. 213–216.
9. **Pei, J., Yue, Z. X., Zhao, F., Li, L. T.** Preparation and Characterization of Citrate Sol-Gel Derived  $\text{Ba}(\text{Zr}, \text{Ti})\text{O}_3$  Ceramics with  $\text{Al}_2\text{O}_3$  Addition *Key Engineering Materials* 336–338 2007: pp. 76–78.
10. **Thongtha, A., Bongkarn, T.** Optimum Sintering Temperature for Fabrication of  $0.8\text{Bi}_{0.5}\text{Na}_{0.5}\text{TiO}_3\text{-}0.2\text{Bi}_{0.5}\text{K}_{0.5}\text{TiO}_3$  Lead-Free Ceramics by Combustion Technique *Key Engineering Materials* 474–476 2011: pp. 1754–1759.
11. **Panya, P., Bongkarn, T.** Fabrication of Perovskite Barium Titanate Ceramics via Combustion Route *Ferroelectrics* 383 2009: pp. 102–110.

12. **Thongtha, A., Bongkarn, T.** Phase Formation and Microstructure of Barium Zirconate Ceramics Prepared Using the Combustion Technique *Ferroelectrics* 383 2009: pp. 33–39.
13. **Panya, P., Vittayakorn, N., Phungjit, N., Bongkarn, T.** The Structural Phase and Microstructure of Perovskite  $\text{Ba}(\text{Ti}_{1-x}\text{Zr}_x)\text{O}_3$  Ceramics Using the Combustion Route *Functional Materials Letters* 2 (4) 2009: pp. 169–174.
14. **Thongtha, A., Angsukased, K., Bongkarn, T.** Fabrication of  $(\text{Ba}_{1-x}\text{Sr}_x)(\text{Zr}_x\text{Ti}_{1-x})\text{O}_3$  Ceramics Using the Combustion Technique *Smart Materials and Structures* 19 2010: pp. 1–7.
15. **Julphunthong, P., Bongkarn, T.** Phase Formation, Microstructure and Dielectric Properties of  $\text{Ba}(\text{Zr}_{0.1}\text{Ti}_{0.9})\text{O}_3$  Ceramics Prepared via the Combustion Technique *Current Applied Physics* 11 (3) 2011: pp. 60–65.
16. **Xu, J., Xue, D., Yan, C.** Chemical Synthesis of  $\text{NaTaO}_3$  Powder at Low-Temperature *Materials Letters* 59 2005: pp. 2920–2922.  
<http://dx.doi.org/10.1016/j.matlet.2005.04.043>
17. **Hwang, C. C., Wu, T. Y., Wan, J., Tsai, J. S.** Development of a Novel Combustion Synthesis Method for Synthesizing of Ceramics Oxide Powders *Materials Science and Engineering: B* 2004: pp. 49–56.
18. Powder Diffraction Files No. 81-2200: International Center for Diffraction data. Newton Square: 2003 PA.
19. **Yu, Z., Ang, C., Guo, R., Bhalla, A. S.** Dielectric Properties of  $\text{Ba}(\text{Ti}_{1-x}\text{Zr}_x)\text{O}_3$  Solid Solutions *Materials Letters* 61 2007: pp. 326–329.  
<http://dx.doi.org/10.1016/j.matlet.2006.04.098>
20. **Smolenskii, G. A., Iagranovskaya, A.** Dielectric Polarization and Losses of Some Complex Compounds *Soviet Physics: Technical Physics* 3 1958: pp. 1380–1382.
21. **Cao, W., Randall, C. A.** Grain Size and Domain Size Relations in Bulk Ceramic Ferroelectric Materials *Journal of Physics and Chemistry of Solids* 57 1996: pp. 1499–1505.
22. **Yimnirun, R., Ananta, S., Laoratanakul, P.** Dielectric and Ferroelectric Properties of Lead Magnesium Niobate–Lead Zirconate Titanate Ceramics Prepared by Mixed-Oxide Method *Journal of the European Ceramics Society* 25 2005: pp. 3235–3242.